Cation Selectivity in Alkali-Exchanged Chabazite: An ab Initio Periodic Study

B. Civalleri,[†] A. M. Ferrari,[†] M. Llunell,[‡] R. Orlando,[§] M. Mérawa,[||] and P. Ugliengo*,[†]

Dipartimento di Chimica IFM, Università di Torino, Via P. Giuria, 7 10125 Torino, Italy, Departament de Química Física, Universitat de Barcelona, Diagonal 647, 08028 Barcelona, Spain, Dipartimento di Scienze e Tecnologie Avanzate, Università del Piemonte Orientale, C.so Borsalino 54, 15100 Alessandria, Italy, and Laboratoire de Chimie Structurale, Unité Mixte de Recherche 5624 au CNRS, Université de Pau, 64000 Pau, France

Received April 18, 2003. Revised Manuscript Received July 5, 2003

Ab initio periodic calculations based on local Gaussian basis sets have been performed to investigate the site preference and cation selectivity of H, Li, Na, and K in Al-substituted high-silica dehydrated chabazite. Two cation sittings were considered: the 6-membered ring (SII) and the 8-membered ring (SIII′) pores. Structures have been fully relaxed at the Hartree−Fock level of theory, and the relative stabilities were verified with density functional single point calculations employing the B3-LYP hybrid functional. Computed ion site preferences for Li and K are in agreement with experimental evidence: Li is more stable at SII whereas K prefers the SIII′ site. For Na, our calculations show that the more stable location is the SII site, at variance with the experimentally observed site preference which depends on the Si/Al ratio. Computed zeolite framework selectivity toward hydrated cations follows the sequence K > Na > Li in line with observed trends. Computed electric field gradients have also been used to evaluate the quadrupolar parameters as a further characterization of the cation positions.

1. Introduction

Zeolites are typically aluminosilicates with an infinite, open, 3-dimensional structure which consists of tetrahedral atoms (T) (Si and Al) linked by oxygen atoms, the so-called TO_4 units. Such TO_4 units are then connected to form multidimensional channels and cages. Aluminum atoms in the framework lead to a net negative charge, and therefore must have extraframework cations associated with them. Alkali and alkaline earth ions are the most commonly encountered cations present in natural zeolites.

The microporous structure and the presence of extraframework cations are of fundamental importance to characterize the unique properties of zeolites. Pores have different shapes and sizes and allow zeolites to be used in separation processes working as molecular sieves.[1] Extraframework cations are weakly bonded and can be removed or exchanged readily with other metal ions. Ion-exchange capacity is a fundamental property of zeolites and leads to important applications in industry as in the removal of ammonia and heavy metals from municipal, industrial, and drinking waters, or in the take-up of Cs and Sr from nuclear waste.[2] Further, cations can effectively act as adsorption sites. Cation-containing zeolites have been demonstrated to be useful in gas separation processes as in the separation of CO_2 from CH_4 or N_2 from O_2.[3] Because of their combination of pores and cations, zeolites have found widespread applications in catalysis. Indeed, their shape selectivity and adsorption capacity play an important role in driving the product formation of many industrial processes such as hydrocarbon conversions in gasoline manufacture and other petrochemical reactions.[4]

Among zeolites, natural and synthetic chabazites have been applied in many industrial processes. Important applications are in gas separation as the vacuum swing adsorption process[3] or in many ion-exchange processes.[5] Alkali and alkaline ions are the most common extraframework cations in chabazites. The location and site preference of such cations has been the target of many experimental works[6] and, recently, alkali ion-exchanged chabazite has been the subject of an extended characterization.[7,8]

* To whom correspondence should be addressed. Phone: +39 011 670 7140. Fax: +39 011 236 7140. E-mail: piero.ugliengo@unito.it.
[†] Università di Torino.
[‡] Universitat de Barcelona.
[§] Università del Piemonte Orientale.
[||] Université de Pau.

(1) Breck, D. W. *Zeolite Molecular Sieves*; Wiley: New York, 1974. (2) Moreno, N.; Querol, X.; Ayora, C. *Environ. Sci. Technol.* **2001**, *35*, 3526. Ouki, S. K.; Kavannagh, M. *Water Sci. Technol.* **1999**, *39*, 115. Mimura, H.; Kobayashi, T.; Akiba, K. *J. Nucl. Sci. Technol.* **1995**, *32*, 60.
(3) Gaffney, T. R. *Curr. Opin. Solid State Mater. Sci.* **1996**, *1*, 69.
(4) Weitkamp, J. *Solid State Ionics* **2000**, *131*, 175.
(5) Torracca, E.; Galli, P.; Pansini, M.; Colella, C. *Micropor. Mesopor. Mater.* **1998**, *20*, 119. Dyer, A.; Zubair, M. *Micropor. Mesopor. Mater.* **1998**, *22*, 135.
(6) Mortier, W. J.; Pluth, J. J.; Smith, J. V. *Mater. Res. Bull.* **1977**, *12*, 241−249. Mortier, W. J.; Pluth, J. J.; Smith, J. V. *Mater. Res. Bull.* **1977**, *12*, 97−102. Alberti, A.; Galli, E.; Vezzalini, G.; Passaglia, E.; Zanazzi, P. F. *Zeolites* **1982**, *2*, 303−309. Caligaris, M.; Mezzetti, A.; Nardin, G.; Randaccio, L. *Zeolites* **1984**, *4*, 323−328. Calligaris, M.; Mezzetti, A.; Nardin, G.; Randaccio, L. *Zeolites* **1986**, *6*, 137−141.

10.1021/cm0342804 CCC: $25.00
Published on Web 09/11/2003

In this work we use a periodic ab initio approach to theoretically investigate the site preference and cation selectivity of H, Li, Na, and K in Al-substituted high-silica chabazite (CHA). The periodic approach was previously applied to model acidic and cation-exchanged zeolites by using both atomistic simulations[9,10] and ab initio calculations.[11−19] Moreover, some of the previous work was especially devoted to study cations in chabazite.[11−14,18]

We adopt the Hartree−Fock (HF) and density functional theory (DFT), the latter based on the hybrid B3-LYP method, within the LCAO approximation and periodic boundary conditions as implemented in the CRYSTAL code.[20] CRYSTAL has already been successfully applied to the study of acidic and cation-exchanged zeolites.[17−19]

Because a zeolitic framework is very flexible due to the low-energy barrier of the T−O−T bridges, it is important to take into account framework relaxations. Recently, on the basis of the implementation in CRYSTAL of the analytical HF nuclear gradient,[21] geometry optimization of periodic systems has become feasible in routine calculations.[22] Our aim, in this work, is to use the new structural optimization capability of the CRYSTAL code to study the relative stability of two different cation sittings, located in the 6-membered ring and in the 8-membrered ring, respectively, for an acidic and alkali-metal exchanged Al-substituted high-silica chabazite. Computed electric field gradient at ^{2}H, ^{7}Li, ^{23}Na, and ^{27}Al nuclei has also been used to characterize the different cation sites.

2. Survey of Experimental Evidence of Cation Location in Chabazite

The chabazite framework is constructed of hexagonal prisms connected by 4-membered ring units to form a 3-dimensional channel system. This produces pores made from 8-membered rings of TO_4 units. The pure-silica form has recently been synthesized.[23] One independent TO_4 unit with four crystallographically different oxygen sites has been observed in the structure and these are indicated in Figure 1. Cation sites in dehydrated and hydrated forms of chabazite have been experimentally studied and the resulting cation sites were characterized.[6−8] These works reveal that three general cation positions exist: one at the center of the hexagonal prism (SI), one at the 6-membered ring window of the prism (SII), and one at the 8-membered ring window either close to the corner of the 4-membered ring of the hexagonal prism or almost at the center of the 8-membered ring (SIII and SIII′, respectively) (see Figure 1).

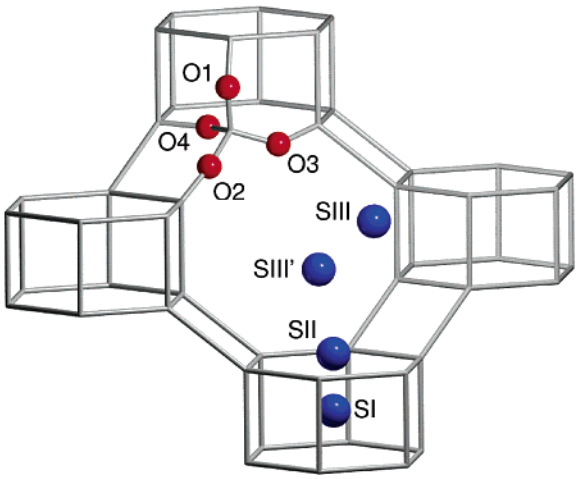

Figure 1. Schematic view of the known cation positions in chabazite. Independent oxygen atoms in the asymmetric unit of the pure silica chabazite are also shown.

Cheetham and co-workers have studied the location of protons[24] and alkali metal cations[7,8] in dehydrated chabazite by the use of neutron powder diffraction, ^{7}Li and ^{23}Na magic-angle spinning (MAS) nuclear magnetic resonance (NMR) spectroscopy, and ^{23}Na multiple quantum MAS (MQMAS) NMR spectroscopy. Experimental results for the acidic chabazite[24] (H−SSZ-13) show the presence of two distinct acid sites in the unit cell, one on the 6-membered ring at O3[25] and one in the 8-membered ring window at O1. For the alkali-chabazites, pure and mixed cation chabazites have been investigated. In Li and Na chabazites no cations were located in the SI site.[7] Instead, cations were found in the other two sittings: at the 6-membered ring window (site SII) and near the 8-membered window close to the corner of the 4-membered ring of the hexagonal prism (site SIII). Unlike Li−CHA, the SIII site in the Na−CHA is displaced almost in the plane of the window; this site has been more properly denominated SIII′ (see Figure 1) according to nomenclature proposed by Cheetham and co-workers.[7,8] In a mixed Li−, Na−, K−CHA, K was found preferentially located at the SIII′ site.[8]

An important aspect to take into account when analyzing experimental measurements is the Si/Al ratio. Indeed, experimental data for alkali-exchanged chaba-

(7) Smith, L. J.; Eckert, H.; Cheetham, A. K. *J. Am. Chem. Soc.* **2000**, *122*, 1700.
(8) Smith, L. J.; Eckert, H.; Cheetham, A. K. *Chem. Mater.* **2001**, *13*, 385.
(9) Higgins, F. M.; Watson, G. W.; Parker, S. C. *J. Phys. Chem. B* **1997**, *101*, 9964.
(10) Grey, T.; Gale, J. D.; Nicholson, D.; Peterson, B. *Micropor. Mesopor. Mater.* **1999**, *31*, 45.
(11) Jeanvoine, Y.; Ángyán, J. G.; Kresse, G.; Hafner, J. *J. Phys. Chem. B* **1998**, *102*, 5573.
(12) Shah, R.; Gale, J. D.; Payne, M. C. *Phase Transitions* **1997**, *61*, 67.
(13) Grey, T.; Gale, J. D.; Nicholson, D.; Artacho, E.; Soler, J. *Stud. Surf. Sci. Catal.* **2000**, *128*, 89.
(14) Barbosa, L. A. M. M.; van Santen, R. A.; Hafner, J. *J. Am. Chem. Soc.* **2001**, *123*, 4530.
(15) Campana, L.; Selloni, A.; Weber, J.; Goursot, A. *J. Phys. Chem. B* **1997**, *101*, 9932.
(16) Benco, L.; Demuth, T.; Hafner, J.; Hutschka, F. *Micropor. Mesopor. Mater.* **2001**, *42*, 1.
(17) Ugliengo, P.; Civalleri, B.; Dovesi, R.; Zicovich-Wilson, C. M. *Phys. Chem. Chem. Phys.* **1999**, *1*, 545.
(18) Ugliengo, P.; Civalleri, B.; Zicovich-Wilson, C. M.; Dovesi, R. *Chem. Phys. Lett.* **2000**, *318*, 247.
(19) White, J. C.; Nicholas, J. B.; Hess, A. C. *J. Phys. Chem. B* **1997**, *101*, 590.
(20) Saunders, V. R.; Dovesi, R.; Roetti, C.; Causà, M.; Harrison, N. M.; Orlando, R.; Zicovich-Wilson, C. M. *CRYSTAL-98 User's Manual*; Università di Torino: Torino, Italy, 1999.
(21) Doll, K.; Harrison, N. M.; Saunders V. R. *Int. J. Quantum Chem.* **2000**, *82*, 1. Doll, K. *Comput. Phys. Comm.* **2001**, *137*, 74.; Orlando, R.; Saunders, V. R.; Dovesi, R.; private communication.
(22) Civalleri, B.; D'Arco, Ph.; Orlando, R.; Saunders, V. R.; Dovesi, R. *Chem. Phys. Lett.* **2001**, *348*, 131.
(23) Diaz-Cabanas, M.-J.; Barrett, P. A.; Camblor, M. A. *Chem. Commun.* **1998**, 1881.
(24) Smith, L. J.; Davidson, A.; Cheetham, A. K. *Catal. Lett.* **1997**, *49*, 143.
(25) Note that in the present work O3 corresponds to O2 in ref 24.

zites refer to a low Si/Al ratio of 2.4 that implies a number of aluminum atoms per unit cell of about 3.5, whereas for the acidic form the Si/Al ratio was determined to be 16. The different Si/Al ratio among chabazites could remarkably affect their physical features. This is because the zeolite−cation interaction results from the subtle interplay of three factors: a weak, but nevertheless attractive covalent bonding between the cation and the framework oxygen atoms; a much stronger attractive electrostatic bonding between the cation and the partially ionic oxygen centers; and a repulsive Coulomb interaction between the cation and the positively charged $Al^{\delta+}$ center.

In the present work, we adopt an Al-substituted high-silica model of chabazite (see below) which contains one Al atom in the unit cell, i.e., the Si/Al ratio is 11:1. This low aluminum content allows a simpler specification of the chabazite models adopted herein and is consistent with the H−SSZ-13 acidic chabazite. However, it makes the comparison with the experimental data for the alkali-exchange chabazites more delicate.

3. Computational Details

3.1. Models. We started from the experimental structure of the pure silica chabazite.[23] Only a crystallographically independent TO_4 unit is present which generates the twelve equivalent tetrahedral units of the unit cell. For simplicity, to create the Al-substituted chabazite, we adopted a Si/Al ratio of 11:1 corresponding to one aluminum atom per unit cell. Because all aluminum atom sites are equivalent, this choice avoids the problem of different Al locations in the framework.

On the basis of the adopted Si/Al loading and the experimental location of the cation sites in chabazites, two cation sittings, hereafter indicated as SII and SIII′, as shown in Figure 1, were then defined as follows. The first step was to define the protonic form of chabazite (H−CHA). The H−CHA had the hydrogen atom linked to the O1 site and was initially fully optimized by means of an atomistic simulation with shell-ion model potentials derived by Sauer and co-workers from ab initio HF calculations on well-designed cluster models.[26,27] Calculations were performed by using the GULP code.[28] Such a level of calculation will be referred to hereafter as GHF. The resulting structure had the proton located in the 8-membered ring window and was used to generate the SIII′ alkali-exchanged chabazites by substituting Li, Na, and K for the hydrogen atom (see Figures 2 and 3). Finally, the hydrogen atom of H−CHA(O1) was moved to be bonded to the O3 atom, as shown in Figure 2. In this way the proton is located in the 6-membered ring window of the hexagonal prism, i.e., the SII site. The proton was then substituted by the alkali-metal ions to create the SII ion-exchanged chabazites (see Figure 3). By keeping the cell parameters fixed as for H−CHA(O1), all the atomic positions of the so-derived ion-exchanged chabazites were then fully relaxed at the adopted level of theory (see below).

Because experimental findings[7] indicate that Li is located in a different position, namely SIII, a model of Li−CHA with a SIII site was also created. However, this site was found to be rather unstable with respect to either SII or SIII′ and it will not be discussed further. An attempt was also made at considering the Na ion located in the SI site (Figure 1). Geometry optimization of that structure showed that the SI cation siting is not a stationary point upon the potential energy surface and the sodium atom moves from the center of the hexagonal prism through the 6-membered ring toward the SII site. We suspect that the instability is due to the low aluminum content of the chabazite models adopted in the present work.

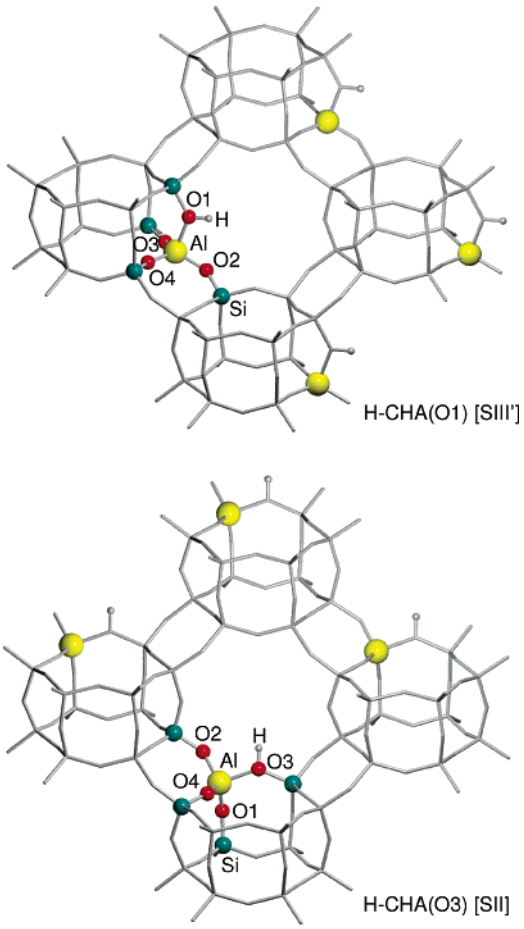

Figure 2. Location of protons in acidic chabazites studied in the present work. Top panel, O1H (corresponding to SIII′ site); bottom panel, O3H (corresponding to SII site). Relevant structural data are reported in Table 1 for the highlighted atoms.

3.2. Methods. Calculations have been carried out at both the HF and DFT levels of theory employing the CRYSTAL code.[20] For DFT calculations Becke's three-parameters hybrid exchange functional[29] in combination with the gradient-corrected correlation functional of Lee, Yang, and Parr,[30] generally referred to as B3LYP, has been used. Considering the largely electrostatic nature of the interactions under study (see also next section), correlation effects are not fundamental for a semiquantitative analysis of the process which can be indeed satisfactorily described at the HF level. However, accurate calculations of the interaction energy obviously require inclusion of correlation effect besides an accurate description of the polarizability of the exchanged cation. In this respect, the B3LYP functional is expected to provide more accurate results. Therefore, the geometry optimization has been performed at the HF level, whereas the energetics of the process has been validated by B3LYP single-point energy calculations. All the structures have been optimized without any symmetry left, i.e., within the P1 space group. A cell-fixed unconstrained optimization of the atomic coordinates was carried out by keeping the cell parameters at the values computed at GHF level for the H−CHA structure with the proton linked to the O1 atom (see above). The forces acting upon the atoms have been obtained by using the recent implementation of analytical HF[21] gradients in CRYSTAL.

(26) Schröder, K.-P.; Sauer, J. *J. Phys. Chem.* **1996**, *100*, 11043.
(27) Sierka, M.; Sauer, J. *Faraday Discuss.* **1997**, *106*, 41.
(28) *GULP (the General Utility Lattice Progam).* Gale, J. D. Royal Institution/Imperial College: UK; 1992−1994. Gale, J. D. *J. Chem. Soc., Faraday Trans.* **1997**, *93*, 629.
(29) Becke, A. D.; *J. Chem. Phys.* **1993**, *98*, 5648.
(30) Lee, C.; Yang, W.; Parr, R. G. *Phys. Rev. B* **1988**, *37*, 785.

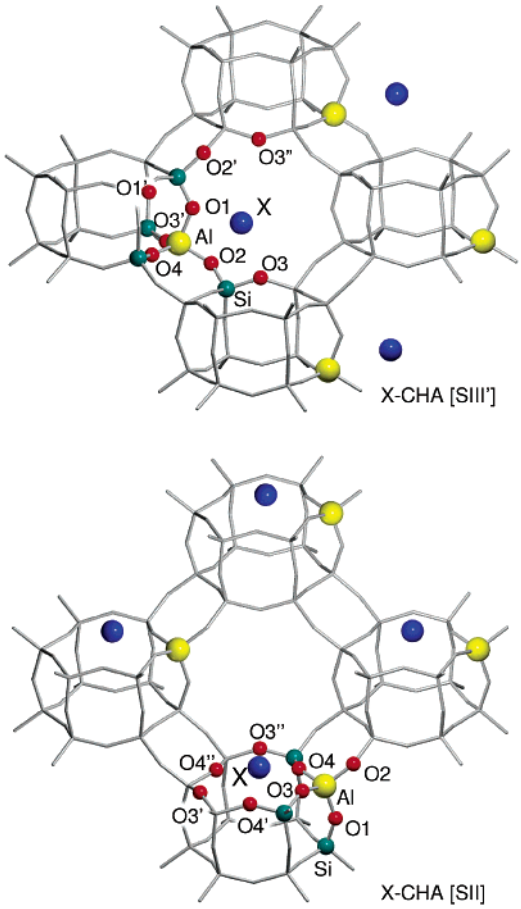

Figure 3. Location of the ions in ion-exchanged chabazites studied in the present work. Top panel, SIII′; bottom panel, SII. Relevant structural data are reported in Table 2 for the highlighted atoms.

These have been used to relax the atoms toward equilibrium using a modified conjugate gradient algorithm as proposed by Schlegel.[31] In the present work, a unit matrix has been used as an initial guess of the Hessian and geometry optimization has been performed in Cartesian coordinates. Convergence was tested on the root-mean-square (RMS) and the absolute value of the largest component of both the gradients and the estimated displacements. In the present calculations the threshold for the maximum and the RMS forces and the maximum and the RMS atomic displacements on all the atoms were set to (in a.u.) 0.00045, 0.00030 and 0.00180, 0.00120, respectively. The optimization was considered complete when all four conditions were satisfied.

6-21G(*d*), 6-31G(*d*), 85-11G(*d*), and 31G(*p*) basis sets have been adopted for Si, O, Al, and H, respectively; the exponents (a.u.), of the most diffuse shells have been optimized ζ_{sp}(Si) = 0.13, ζ_{sp}(O) = 0.27, ζ_{sp}(Al) = 0.28; the exponent of the polarization functions are ζ_d(Si) = 0.5, ζ_d(O) = 0.6, ζ_d(Al) = 0.47, ζ_p(H) = 1.1; *d* shells are represented by five functions. These basis sets have been used successfully in the characterization of the acidic form of zeolites.[17,18] For the alkali metal atoms the following basis sets have been used: 6-1G for Li, 8-511G for Na, and 86-511G for K.[32] The number of reciprocal lattice points (*k*-points) at which the Hamiltonian matrix has been diagonalized is 8, corresponding to a shrinking factor *S* = 2.[20] Default tolerances for the integrals calculations were adopted at HF and DFT levels of theory, as well as default grids for numerical integration in DFT calculations.[20]

(31) Schlegel, H. B. *J. Comput. Chem.* **1982**, *3*, 214.
(32) Dovesi, R.; Roetti, C.; Freyria-Fava, C.; Prencipe, M.; Saunders, V. R. *Chem. Phys.* **1991**, *156*, 11.

Table 1. Relevant Structural Data (Bond Lengths in Å, Angles in Degrees) for Acidic Chabazites Computed at HF Level[a]

data[b]	H−CHA(O3) [SII]	H−CHA(O1) [SIII′]
O_b−H	0.952	0.950
Al−H	2.405	2.417
Al−O_b	1.911	1.914
Si−O_b	1.706	1.696
Al−O1−Si	144.7	133.0
Al−O2−Si	143.7	145.5
Al−O3−Si	137.0	159.2
Al−O4−Si	148.5	154.4
Al−O_b(H)−Si	8.4	5.6

[a] See text and Figure 2 for further details. [b] O_b indicates the oxygen atom linked to the proton, i.e., either O1 or O3.

It is worth noting that calculations typically consisted of 557−569 basis functions and have been performed by the use of a direct SCF technique for two-electron integrals. Under such conditions, geometry optimizations (108 degrees of freedom) required from 3−4 days of CPU time on a Linux PC with a 1.1 GHz Athlon processor and 1 GB of memory.

The electric field gradient (EFG) computed from the B3-LYP wave functions has been evaluated at the HF optimized nuclear positions of the different ion-exchanged chabazite structures. From the computed EFG the so-called quadrupolar parameters can be obtained: the nuclear quadrupole coupling constant (NQCC), q_{cc},

$$q_{cc}(A)=\frac{eQ(A)}{h}V_{zz}(A) \qquad (1)$$

and the asymmetric parameter, η,

$$\eta(A)=\frac{V_{xx}(A)-V_{yy}(A)}{V_{zz}(A)} \qquad (2)$$

Here, $eQ(A)$ is the electric quadrupole moment of the nucleus *A*, *h* is the Planck's constant, and V_{ii} are the eigenvalues of the traceless EFG tensor at the position of nucleus *A*. The principal axis system for the EFG tensor is chosen such that $|V_{zz}(A)| > |V_{yy}(A)| > |V_{xx}(A)|$, whereby $0 < \eta < 1$. Electric quadrupole moments are taken from ref 33 (in bars): ^{7}Li = −0.0401, ^{23}Na = 0.104, ^{2}H = 0.00286, and ^{27}Al = 0.1466. Conversion factors to compute the nuclear quadrupolar coupling constant (in MHz/a.u.) are then ^{7}Li = −9.422, ^{23}Na = 24.44, ^{2}H = 0.6720, and ^{27}Al = 34.45.

4. Results and Discussion

4.1. Cation Location and Structure. Relevant structural data of the studied acidic and alkali exchanged chabazites are reported in Tables 1 and 2. Here, we briefly discuss the main features that characterize each chabazite structure.

4.1.1. Acidic Chabazite. As described in the Models section above, alkali cations in exchanged chabazite have been located in proximity of the positions formally occupied by hydrogen in the corresponding protonated form of chabazite (H−SSZ-13). Experimental data for this high Si/Al ratio acidic chabazite[24] indicate that protonation occurs only at the O1 and O3 sites[25] with a site occupancy at O1 similar to that of the O3 location (Figure 2). For this reason inspection of protonated forms has been limited to these two more frequently occurring structures. In the H−CHA(O1) chabazite the proton points toward the center of the 8-membered window almost in the plane of the ring (d(O1−H) =

(33) Pyykko, P. *Mol. Phys.* **2001**, *99*, 1617.

Table 2. Relevant Structural Data (Bond Lengths in Å, Angles in Degrees) for Alkali-Metal Chabazites Computed at HF Level[a]

site	data	X = Li^+	X = Na^+	X = K^+
SII	X−Al	2.669	3.131	3.531
	X−O3	1.999	2.503	2.888
	X−O4	1.910	2.289	2.739
	X−O4′	2.099	2.396	2.845
	X−O3′	3.348	3.107	3.233
	X−O3″	3.398	3.005	3.221
	X−O4″	2.906	2.548	2.924
	Al−O1−Si	145.3	145.4	145.2
	Al−O2−Si	154.8	150.2	146.7
	Al−O3−Si	147.8	146.3	144.7
	Al−O4−Si	135.5	142.5	147.8
	O3−Al−O4	94.1	99.0	102.3
	O3−Al−O4−X	−1.9	0.2	−13.2
	Si−Al−Si−X	17.3	20.9	34.5
SIII′	X−Al	2.577	3.044	3.725
	X−O1	1.849	2.312	2.814
	X−O2	1.881	2.316	3.092
	X−O2′	3.490	3.627	3.473
	X−O3	2.911	2.718	3.165
	X−O3′	4.105	3.879	3.227
	X−O4	3.836	4.319	5.020
	Al−O1−Si	132.7	133.7	136.9
	Al−O2−Si	141.4	143.7	143.5
	Al−O3′−Si	153.4	153.8	152.8
	Al−O4−Si	152.5	152.9	152.8
	O1−Al−O2	92.4	97.9	101.0
	O1−Al−O2−X	−5.8	−7.2	−8.7

[a] See text and Figure 3 for further details.

0.950 Å). In the case of the H−CHA(O3) chabazite the proton is oriented toward the center of the supercage and the 8-membered ring almost perpendicular to the plane of the 6-membered ring (d(O3−H) = 0.952 Å), as shown in Figure 2. This is at variance with neutron diffraction evidence, which reveals that the proton is tilted toward the center of the 6-membered ring at an angle of 45° from the plane of the Si−O−Al bridge. Further checks, starting from strongly nonplanar Si−O(H)−Al moieties always converged to a slightly nonplanar geometry with the computed Si−O(H)−Al dihedral angle of 5.6 and 8.4 for SIII site and SII site, respectively.

4.1.2. Lithium Chabazite. According to the present calculations the favored location of Li cations in chabazite is the SII site (see next section). At this structural position Li cations are placed at the corner of the 6-membered window of the hexagonal prism (Figure 3), almost bridged at the O3−Al−O4 2-fold site as indicated by the short Li−oxygen bond distances, d(Li−O3) = 1.999 Å, d(Li−O4) = 1.910 Å and the small O3−Al−O4 angle of 94.1°, as reported in Table 2. As an indication of the cation location within the 6-membered ring the Si−Al−Si−X dihedral angle has been reported in Table 2. For Li−CHA a value of 17.3° was computed showing that Li lies slightly above the plane of the ring. Unlike the present investigation, experimental results indicate that Li cations lie almost at the center of the 6-membered ring characterized by short Li−oxygen bond distances with the oxygen centers oriented inward the ring, d(Li−O4) = 1.960 Å, and longer bond distances with the oxygen centers oriented outward the ring, d(Li−O3) = 2.986 Å. Such a discrepancy can be easily explained in terms of structural differences between computed and synthesized chabazite due to the lower Si/Al ratio of the latter. Some support to the role of the Al loading comes from a recent density functional cluster model study showing that the exact location of small cations in a 6-membered ring of faujasite zeolites indeed depends on the number of aluminum atoms in the ring;[34] for 6-membered rings with two or three aluminum atoms, cations interact mainly with the oxygen atom directed inward the ring and are located almost at the center of the ring, whereas in the case of a ring with only one aluminum atom the cations are situated near the oxygen atoms involved in the Al−O−Si bridges in agreement with present results.

At site SIII′ Li cations are located at the corner of the 8-membered ring (Figure 3) bridged at the O1−Al−O2 2-fold site. Li is close to the Al−O−Si bridges with Li−O distances of d(Li−O1) = 1.849 Å and d(Li−O2) = 1.881 Å, shorter than those of the SII site, as reported in Table 2. The O1−Al−O2 angle is in this case 92.4°.

4.1.3. Sodium Chabazite. At SII, Na cations are placed almost at the center of the 6-membered ring of the hexagonal prism with a bond distance to the nearest oxygen d(Na−O3) of 2.289 Å and at a distance from the two next nearest coordinating oxygen atoms d(Na−O4′) = 2.396 Å and d(Na−O3″) = 2.503 Å. With respect to Li, Na lies higher above the plane of the 6-membered ring, with a Si−Al−Si−X angle of 20.9°; accordingly, the computed O4−Al−O3 angle is also larger, being equal to 99.4°. At SIII′ sites Na cations are located at the corner of the 8-membered ring bridged at the O1−Al−O2 2-fold site (d(Na−O1) = 2.312 Å and d(Na−O2) = 2.316 Å, Table 2) in excellent agreement with the experimental value of 2.32 Å. Because Na is located farther than Li from the Al−O−Si bridges, the O1−Al−O2 angle increases to 97.9°.

4.1.4. Potassium Chabazite. Because of the increased dimension, K cations do not fit the 6-membered ring at SII site and lie considerably above the plane of the ring in the supercage; the Si−Al−Si−X angle is now 34.5°, while the O4−Al−O3 angle increases to 102.3. Potassium is placed almost at the center of the 6-membered ring with averaged shorter bond distance from the oxygen atoms directed inward the ring (d(K−O4) = 2.739 Å, d(K−O4′) = 2.845 Å, and d(K−O4″) = 2.924 Å, Table 2). A better accommodation is possible at SIII′ site, in the 8-membered ring, where K cations lie in the plane of the ring and can favorably interact with the nearest oxygen atoms. They are located at the O1−Al−O2 2-fold site corner (d(K−O1) = 2.814 Å, d(K−O2) = 3.092 Å, d(K−O3) = 3.165 Å, and d(K−O3′) = 3.221 Å) not far from the center of an 8-membered ring. Experimental works on mixed Li−Na−K chabazites[8] reveal that the K ion lies almost at the center of the 8-membered window in agreement with data reported in Table 2.

4.2. Cation Location and Relative Stability. The relative stability of the two cation sittings is reported in Table 3. The H−CHA(O1) form of chabazite (SIII′ site) is more favored over the H−CHA(O3) form (SII site) by 11.2 and 6.9 kJ/mol at the HF and B3LYP//HF level, respectively, in agreement with experimental indications[24] and previous high-quality calculations.[11,12,35]

(34) Vayssilov, G. N.; Staufer, M.; Belling, T.; Neyman, K. M.; Knözinger, H.; Rösch, N. *J. Phys. Chem. B* **1999**, *103*, 7920.

(35) Brandle, M.; Sauer, J.; Dovesi, R.; Harrison, N. M. *J. Chem. Phys.* **1998**, *109*, 10379.

Table 3. HF and B3LYP//HF (in parentheses) Relative Stability of SIII′ Site with Respect to SII Site and Energy of Formation from Oxides (α-Quartz, α-Alumina, X_2O (X = H, Li, Na, K)) of Acidic and Alkali Metals Chabazites for the Two Cation Sittings, SII and SIII′[a]

cation	$\Delta E_{SIII'-SII}$	ΔE_{form}(SII)	ΔE_{form}(SIII′)
H	−11.2 (−6.9)	103.0 (119.4)	91.8 (112.5)
Li	7.9 (9.2)	24.4 (59.2)	32.2 (68.5)
Na	10.7 (12.5)	−88.1 (−41.5)	−77.4 (−29.1)
K	−18.3 (−18.1)	−218.8 (−173.8)	−237.1 (−191.9)

[a] See text for further details. Data in kJ/mol.

The most stable cation position in Li−CHA is the SII site. In disagreement with experimental findings,[7] where Li ions were observed in the SII and SIII positions, location of Li cations at site SIII (not reported in Table 2) results to be considerably less favored by about 39.5 and 38.4 kJ/mol at the HF and B3LYP//HF levels, respectively. Surprisingly, site SIII′ is only 7.9 and 9.2 kJ/mol less stable than SII at the HF and B3LYP//HF levels, respectively.

SII is also the preferred site in the case of Na cations being more stable than SIII′ by 10.7 and 12.5 kJ/mol at the HF and B3LYP//HF levels, respectively. The definite preference of Na cations for SII sites reported in this work (similar to that computed for Li ions, Table 3), has been only partially confirmed by experimental observations. Indeed, in a mixed Li−Na chabazite, whereas Li cations show a complete selectivity toward SII, Na ions occupy SII sites only after saturation of SIII′ sites; even in a pure Na−CHA, an incomplete occupation of SII was observed, with the remaining Na cations located at the eight window sites.[6,7] In the case of a Si/Al ≥ 3 an almost full occupancy of SII had been suggested, but with a minor occupancy of SIII′ in order to minimize cation repulsion.[6] The comparison between experimental and computed results, as already stressed, is not straightforward because the occupancy is a function of the Si/Al ratio.

Unlike the location of Na and Li cations, the location of K ions at the SIII′ site is remarkably favored than at the SII site by 18.3 and 18.1 kJ/mol at the HF and B3LYP//HF levels, respectively. This is due to the increased dimension of the K cation which does not fit the 6-membered ring and is more conveniently accommodated in the 8-membered ring. The SIII′ site preference for K ions has been experimentally evidenced: X-ray and neutron diffraction data for binary Li−K−CHA and Na−K−CHA, and ternary Li−Na−K−CHA always show that K cations reside primarily at the SIII′ sites for all the investigated K ions percentages.[8]

4.3. Acidic and Alkali-Exchanged Chabazite Energy of Formation. Table 3 also reports the energy of formation per formula unit of each ion-exchanged chabazite from the corresponding oxides, evaluated in the reactions

$$11\ SiO_2\,(\alpha\text{−quartz})\,(s) + 1/2\ \alpha\text{−}Al_2O_3\,(s) + 1/2\ H_2O\,(g) \rightarrow HAlSi_{11}O_{24}\quad (H\text{−CHA})\quad (1)$$

$$11\ SiO_2\,(\alpha\text{−quartz})\,(s) + 1/2\alpha\text{−}Al_2O_3\,(s) + 1/2X_2O(s) \rightarrow XAlSi_{11}O_{24} (X\text{−CHA}, X = Li, Na, K)\quad (2)$$

which represent the transformation of corundum α-Al_2O_3 and α-quartz, in the presence of either water or alkali-metal oxides, to give the final ion-exchanged CHA with the desidered Si/Al ratio. The resulting energies of formation, even if not meaningful on an absolute scale, show the definite endothermicity of the reactions for H and Li for both cation sites, whereas the formation of Na and K chabazites from oxides is exothermic. The energetics change if pure silica chabazite is considered as a reference instead of α-quartz. The formation energy of H−CHA still would be endothermic, whereas the formation of Li−CHA would become exothermic.

Actually, for H−CHA, reaction 1 should be referred to $H_2O(l)$ instead of $H_2O(g)$. Thus, the $H_2O(g) \rightarrow H_2O(l)$ enthalpy of vaporization ($\Delta H_{vap,m}$ = 46 kJ/mol) has to be included in the thermochemistry, and an energy cost of −23 kJ/mol has to be added to the computed energy of formation. Nevertheless, even if this correction is applied, the energy of formation of H−CHA is still endothermic.

Computed HF formation energies for alkali-chabazites satisfactorily compare with estimates of the experimental enthalpy of formation of dehydrated chabazite from oxides,[36] ΔE_{form}(K−CHA) ≈ −230 kJ/mol, ΔE_{form}(Na−CHA) ≈ −71 kJ/mol, and ΔE_{form}(Li−CHA) ≈ −32 kJ/mol at least for the K and Na exchanged zeolites (these numbers have been obtained by extrapolating experimental data from ref 36 to a Si/Al ratio of 11:1). Discrepancy for Li−CHA can be imputed to difficulties in correctly modeling the site preference of Li cations in chabazite. In any case, these formation energies cannot be directly connected to the selectivity of the zeolite toward the alkali cations because they also depend on the relative stabilities of alkali oxides. B3LYP//HF calculations show that electron correlation reduces the formation energies, the data all being smaller than the HF values by some 35−45 kJ/mol. Remarkably, the trend computed at HF level is not affected by B3LYP correction.

4.4. Cation Selectivity and Ion Exchange. A direct evaluation of the cation selectivity would require the computation of the energy balance involved in the following reaction:

$$CHA^- + X^+ \rightarrow X\text{−CHA}\quad X = Li, Na, K\qquad (3)$$

Unfortunately, such a calculation is not easily accessible for an infinite system because of the charged nature of the zeolite substrate, CHA^-.

Cation selectivity in periodic systems can be more conveniently derived by considering ion exchange reactions. The most simple ion exchange process is

$$X\text{−CHA}(s) + Y^+(g) \rightarrow Y\text{−CHA}(s) + X^+(g)\quad X, Y = H, Li, Na, K\quad (4)$$

where naked cations are considered. Computed HF and B3LYP//HF results are reported in Table 3. The alkali cation selectivity in chabazite as derived by data of Table 3 follows the sequence Li > Na > K. This is in agreement with calorimetric data[36] (enthalpy of formation from elements at 25 °C of hydrated chabazites, with a Si/Al ratio around 3, are −15 380 kJ/mol for LiCHA, −15 235 kJ/mol for NaCHA, and −14 530 kJ/mol for KCHA).

(36) Shim, S.-H.; Navrotsky, A.; Gaffney, T. R.; MacDougall, J. E. *Am. Mineral.* **1999**, *84*, 1870.

Table 4. HF and B3LYP//HF (in parentheses) Energy of Ion-Exchange ΔE_{ex} (in kJ/mol)[a]

	naked cation				hydrated cation [b]				cation hydride			
SII→SII	$HCHA_{II}$	$LiCHA_{II}$	$NaCHA_{II}$	$KCHA_{II}$	$HCHA_{II}$	$LiCHA_{II}$	$NaCHA_{II}$	$KCHA_{II}$	$HCHA_{II}$	$LiCHA_{II}$	$NaCHA_{II}$	$KCHA_{II}$
$HCHA_{II}$	0.0	670 (657)	745 (724)	826 (810)	0.0	100 (87)	60 (39)	62 (45)	0.0	−421 (−432)	−451 (−458)	−486 (−497)
$LiCHA_{II}$		0.0	74 (68)	156 (153)		0.0	−41 (−47)	−39 (−42)		0.0	−30 (−27)	−65 (−65)
$NaCHA_{II}$			0.0	82 (85)			0.0	2 (−5)			0.0	−35 (−38)
$KCHA_{II}$				0.0				0.0				0.0
SIII′→SIII′	$HCHA_{III'}$	$LiCHA_{III'}$	$NaCHA_{III'}$	$KCHA_{III'}$	$HCHA_{III'}$	$LiCHA_{III'}$	$NaCHA_{III'}$	$KCHA_{III'}$	$HCHA_{III'}$	$LiCHA_{III'}$	$NaCHA_{III'}$	$KCHA_{III'}$
$HCHA_{III'}$	0.0	690 (673)	767 (744)	819.5 (798)	0.0	120 (103)	82 (59)	54.5 (33)	0.0	−401 (−416)	−428 (−439)	−492 (−508)
$LiCHA_{III'}$		0.0	77 (71)	130 (126)		0.0	−38 (−44)	−65 (−69)		0.0	−27 (−24)	−91 (−92)
$NaCHA_{III'}$			0.0	53 (55)			0.0	−27 (−25)			0.0	−64 (−69)
$KCHA_{III'}$				0.0				0.0				0.0
SII→SIII′	$HCHA_{III'}$	$LiCHA_{III'}$	$NaCHA_{III'}$	$KCHA_{III'}$	$HCHA_{III'}$	$LiCHA_{III'}$	$NaCHA_{III'}$	$KCHA_{III'}$	$HCHA_{III'}$	$LiCHA_{III'}$	$NaCHA_{III'}$	$KCHA_{III'}$
$HCHA_{II}$	−11 (−7)	682 (663)	756 (731)	838 (816)	−11 (−7)	112 (93)	71 (46)	73 (51)	−11 (−7)	−413 (−422)	−440 (−446)	−505 (−515)
$LiCHA_{II}$		8 (9)	66 (59)	148 (144)		8 (9)	−49 (−56)	−47 (−51)		8 (9)	−19 (−14)	−83 (−83)
$NaCHA_{II}$			11 (12)	71 (73)			11 (12)	9 (7)			11 (12)	−53 (−56)
$KCHA_{II}$				−18 (−19)				−18 (−19)				−18 (−19)
SIII′→SII	$HCHA_{II}$	$LiCHA_{II}$	$NaCHA_{II}$	$KCHA_{II}$	$HCHA_{II}$	$LiCHA_{II}$	$NaCHA_{II}$	$KCHA_{II}$	$HCHA_{II}$	$LiCHA_{II}$	$NaCHA_{II}$	$KCHA_{II}$
$HCHA_{III'}$	11 (7)	678 (666)	755.5 (737)	808 (792)	11 (7)	108 (96)	70 (52)	43 (27)	11 (7)	−408 (−425)	−438 (−452)	−474 (−490)
$LiCHA_{III'}$		−8 (−9)	85 (80)	138 (135)		−8 (−9)	−30 (−35)	−57 (−60)		−8 (−9)	−38 (−36)	−73 (−74)
$NaCHA_{III'}$			−11 (−12)	63.5 (67)			−11 (−12)	−16.5 (−13)			−11 (−12)	−46 (−51)
$KCHA_{III'}$				18 (19)				18 (19)				18 (19)

[a] Data refer to the reaction $X{-}CHA_Z(s) + Y^+(g) \rightarrow Y{-}CHA_Z(s) + X^+(g)$ with X (Y) = H, Li, Na, K, and Z = II, III′. See text for further details. [b] Values derived employing experimental hydration energy from ref 37.

This sequence differs from that derived by ion exchange experiments with chabazite in aqueous media in which selectivity is reversed, i.e., K > Na.[5] Data obtained from eq 4 are relative to a gas-phase process and cannot account for the observed trend because the binding preference for Na^+ or K^+ depends on solvent polarity. Selectivity is inherently a delicate balance between the forces the cation experiences within the zeolite framework with respect to the solvent molecules. To investigate the role of aqueous media, we have then examined the exchange reaction

$$X{-}CHA(s) + Y^+_{hydrated} \rightarrow Y{-}CHA(s) + X^+_{hydrated} \quad X, Y = H, Li, Na, K \quad (5)$$

where data concerning hydrated cations have been taken from experimental measurements.[37] Results from eq 5 are reported in Table 3. Cation selectivity now shows a reversed tendency (Li < Na < K) in better agreement with observations.[5] Only a qualitative comparison with the experimental trend can be done because computed data on cation-exchanged chabazites should refer to the fully hydrated zeolites. However, for the Na−CHA (SII) → K−CHA (SIII′) reaction, the B3LYP//HF exchange energy $\Delta E_{ex} = -7.3$ kJ/mol (Table 3) is of the same order of magnitude of the experimental exchange free energy $\Delta G_{ex} = -5.2$ kJ/mol reported in ref 5.

According to the computed values for reactions 4 and 5, (Table 3), protonated chabazite should be the most stable form. Natural zeolites exist mainly in the Na form with other alkali and earth alkaline metals as impurities. The protonated form is prepared after exchanging the cations with NH_4^+ and successively heating the product in vacuo.[24] High-quality calculations combining quantum mechanics and shell-ion model potential have determined the binding energy involved in the processes $CHA^- + H^+ \rightarrow H{-}CHA$ and $CHA^- + NH_4^+ \rightarrow NH_4{-}CHA$ that are −1273 and −484 kJ/mol, respectively,[35] showing a clear preference for the protonated form H−CHA. The isothermal value of −789 kJ/mol for the reaction $HCHA + NH_4^+ \rightarrow NH_4CHA + H^+$ is close to the values of −744 and −798 kJ/mol reported in Table 3 for the exchange reactions $HCHA + X^+ \rightarrow XCHA + H^+$ with X = Na and K. This trend compares well with the experimental selectivity:[5] $NH_4^+ > K^+ > Na^+$.

From a different point of view, cation exchange in zeolites can also be performed by adopting the so-called *solid-state ion exchange* technique.[38] The exchange is usually performed by mixing a salt with the zeolite, and following that with long heating. The salt decomposes and can be transported into the zeolitic channels/cages either in the form of whole molecules or after the separation of cations and anions. In the former case, a whole molecule diffuses and an exchange reaction between the extraframework cations and the incoming one finally occurs. In particular, this technique has been adopted specifically to exchange protonic forms of zeolites. Usually, metal chloride salts are used: recently, in our laboratory a Li−ZSM-5 has been prepared by exchanging H−ZSM-5 with LiH.[39] The reaction not only gives rise to Li−ZSM-5, but also evolution of molecular H_2 is observed. This prompted us to also consider the following ion exchange reaction:

$$X{-}CHA(s) + YH(g) \rightarrow Y{-}CHA(s) + XH(g) \quad X = H, Li, Na, K; Y = Li, Na, K \quad (6)$$

Because both reactants and products can be computationally studied on the same basis, such a reaction offers a valuable means to characterize the cation selectivity. The resulting computed ion exchange energies are reported in Table 4. Unlike previous ion

(37) Heat of hydration (M^+ (g), in kJ/mol): $H^+ = 1090$, $Li^+ = 520$, $Na^+ = 405$, $K^+ = 325$. Taken from Greenwood, N. N.; Earnshow, A. *Chemistry of Elements*, 2nd ed.; Butterworth-Heinemann: Oxford, 1997.

(38) Karge, H. G. In *Progress in Zeolite and Microporous Materials*; Chon, H., Ihm, S.-K., Uh, Y. S., Eds.; Studies in Surface Sciences and Catalysis, Vol. 105; Elsevier: Amsterdam, The Netherlands, 1997; Part C, p 1901.

(39) Llabrés i Xamena, F. X.; Zecchina, A.; private communication.

Table 5. X−CHA (X = H, Li, Na) B3LYP//HF: Nuclear Quadrupolar Coupling Constants, q_{cc} (in MHz) and Asymmetric Parameters, η

	SII		SIII′	
atom	q_{cc}	η	q_{cc}	η
^{2}H	0.334	0.11	0.339	0.09
^{7}Li	0.315	1.00	0.304	0.94
^{23}Na	4.8	0.43	4.4	0.28

exchange reactions, now the protonic form of chabazite is no longer the most stable one. Results in Table 4 also show that this kind of ion exchange is particulary efficient to exchange protons, but it is less selective when different cations are involved. The energy for proton exchange is almost an order of magnitude larger than that for alkali metal ions and the computed trend in selectivity is now K > Na > Li > H.

4.4. Electric Field Gradient and NQCC. As an additional source of information on the cation sites, the electric field gradient (EFG) at the H, Li, Na, and Al nuclei has been calculated for both SII and SIII sites of the considered chabazites. Because the electric field gradient depends on the local symmetry of the cation environment, it offers a means to characterize the different cation locations.

Computed B3LYP//HF quadrupolar parameters for ^{2}H, ^{7}Li, and ^{23}Na are reported in Table 5. In the acidic chabazite, they are quite similar for both sites. This is in agreement with the general trend observed in acidic zeolites with different frameworks and Si/Al loadings.[40] Indeed, the experimental range for q_{cc} is rather narrow, varying from 236 to 208 kHz, and the same holds for η, which varies from 0.06 to 0.15. In comparison with these data, B3LYP//HF computed NQCCs are slightly overestimated.

NQCC values for Li−CHA are 315 kHz, with $\eta = 1.00$, for SII, and 304 MHz, with $\eta = 0.94$, for the SIII site. Experimentally, the SII site is characterized by a NQCC of 280 kHz with $\eta = 0.3$, whereas for the SIII site a NQCC of 240 kHz with $\eta = 1.0$ is observed.[7] Computed and observed nuclear quadrupole coupling constants are in good agreement, whereas some discrepancy is seen for the η value at site SII. In this respect, one should bear in mind that η describes the asymmetry of the electric field gradient tensor, and, therefore, it is extremely sensitive to the surroundings of the cation position. Differences between computed and observed η may reflect the different environment of Li cation in the 6-membered ring, which lies almost in the center of the ring in synthesized chabazite, whereas it is predicted to be displaced toward the corner of the 6-membered ring by the present calculations.

For Na−CHA, computed values for SII are NQCC = 4.8 MHz and $\eta = 0.43$, whereas for the SIII site it results in NQCC = 4.4 MHz and $\eta = 0.28$, in satisfactory agreement with experiment[7] (for the SII site ^{23}Na−NQCC = 5.1 MHz and $\eta = 0.1$, while ^{23}Na−NQCC is ranging from 3.6 to 4.1 MHz with $0.4 < \eta < 1.0$ for the SIII′ site, due to aluminum disorder in the tetrahedral positions).

The q_{cc} and η for ^{27}Al in the ion-exchanged chabazites are gathered in Table 6. A comparison among computed and experimental data is at hand for acidic and Na-containing zeolites. Observed q_{cc} for ^{27}Al in acidic zeolites[40] varies from 10.8±1.0 to 16.0±1.0 MHz and the corresponding η values are from 0.9±0.1 to 0.1±0.1. In H−CHA, computed data for the two proton positions are quite close to each other: 19.1 MHz (0.31) and 21.2 MHz (0.30), in which the asymmetric parameter is reported in parentheses. These values agree favorably with experimental data for a high silica H−ZSM-5 (Si/Al = 22±1): $q_{cc} = 16.0 \pm 1.0$ MHz, $\eta = 0.1 \pm 0.1$. Experimental data[40] are also available for various Na-zeolites. In this case, quadrupole parameters range from 5.5±1.0 MHz (0.3±0.1) to 4.7±1.0 MHz (0.5±0.1) values. The latter values correspond to a high silica Na−ZMS-5 and are in good agreement with our results for ^{27}Al in Na−CHA (see Table 6). In general, an almost linear decreasing can be observed in the q_{cc} values going from Li to K for both SII and SIII′. This probably depends on the charge of the framework oxygen atoms coordinating the alkali-metal ion. Indeed, the basicity of the surrounding oxygens decreases from Li to K.

Table 6. B3LYP//HF ^{27}Al Nuclear Quadrupolar Coupling Constants, q_{cc} (in MHz) and Asymmetric Parameters, η, for X−CHA (X = H, Li, Na, K)

^{27}Al	SII		SIII′	
cation	q_{cc}	η	q_{cc}	η
H	19.1	0.31	21.2	0.30
Li	10.2	0.60	10.4	0.74
Na	7.6	0.65	6.9	0.89
K	5.8	0.80	5.1	0.72

Computed data for Li and Na permit clear discrimination between the two cation positions. For H−CHA, computed quadrupolar parameters seem to be insufficient to give precise information on the two proton locations. In this case, other typical features such as the ν(OH) vibrational frequency might be fruitfully used to discriminate between O1−H and O3−H.

5. Conclusions

Periodic ab initio calculations have been perfomed to investigate the cation location and relative stability of two different sites (SII and SIII′) in a protonated and alkali-exchanged Al-substituted high silica chabazite. Different ion exchange reactions have been studied to evaluate a cation selectivity scale. Structural relaxation has been taken into account by geometry optimization of the atomic positions at the Hartree−Fock level of theory. Refinement of the energetics has been carried out by B3-LYP single-point energy calculations on the HF optimized structures. The main conclusions are summarized as follows. (1) The effect of electron correlation has found to be relatively modest as a semiquantitative agreement between HF and B3LYP//HF energetics has always been obtained. (2) Cation site preference is in reasonable agreement with experiment: Li at SII, K at SIII′. A more delicate situation occurs for Na: calculations show a preference for SII, whereas experimental evidence reveals a dependence on the zeolite Si/Al ratio.[7] However, the moderate preference for SII over SIII′ (about 10 kJ/mol) is compatible with the behavior occurring in the experimental situation. Incidentally, it is worth noting that the location of lithium is similar to the observed cation

(40) Freude, D.; Ernst, H.; Wolf, I. *Solid State Nucl. Magn. Res.* **1994**, *3*, 271.

location in zeolite X (e.g., see ref. 41 and references therein). (3) Cation selectivity strongly depends on the considered ion exchange reaction. A sequence Li > Na > K has been computed by considering naked cations, while a reversed trend Li < Na < K has been obtained for hydrated cations, in line with observations for reactions occurring in aqueous media. When ion exchange reactions 4 and 5 are adopted, results indicate a stronger stability of protonated chabazite compared to the alkali exchanged form. However, when a solid-state ion exchange reaction is considered, the cation selectivity order K > Na > Li > H is obtained. Direct comparison with experiment is not possible because of the lack of specific data, even if reaction 6 seems to be ideally suited for comparison between computed and experimental results. (4) B3-LYP//HF nuclear quadrupole coupling constants, q_{cc}, and the asymmetry parameters, η, of the electric field gradient data are in fairly good agreement with the experimental values. Small discrepancies can be imputed to structural differences between synthesized and modeled chabazite mainly due to the different Al/Si ratio and to the local structure of cation sites which has a significant influence on the computed quadrupolar parameters.

Acknowledgment. The present work is part of a project coordinated by A. Zecchina and cofinanced by the Italian MURST (Cofin98, Area 03). We also acknowledge the CINECA for a high-performance computing grant. M.M. acknowledges support by CNRS and MESR, and computing resources from CINES.

CM0342804

(41) Feuerstein, M.; Engelhardt, G.; McDaniel, P. L.; MacDougall, J. E.; Gaffney, T. R. *Microporous Mesoporous Mater.* **1998**, *26*, 27.